



Optics Letters

Engineering the spectral bandwidth of quantum cascade laser frequency combs

MAXIMILIAN BEISER,[†]  NIKOLA OPAČAK,[†]  JOHANNES HILLBRAND,[†]  GOTTFRIED STRASSER,[†] 
AND BENEDIKT SCHWARZ* 

Institute of Solid State Electronics, TU Wien, 1040 Vienna, Austria

*Corresponding author: benedikt.schwarz@tuwien.ac.at

Received 8 March 2021; revised 8 May 2021; accepted 11 May 2021; posted 20 May 2021 (Doc. ID 424164); published 14 July 2021

Quantum cascade lasers (QCLs) facilitate compact optical frequency comb sources that operate in the mid-infrared and terahertz spectral regions, where many molecules have their fundamental absorption lines. Enhancing the optical bandwidth of these chip-sized lasers is of paramount importance to address their application in broadband high-precision spectroscopy. In this work, we provide a numerical and experimental investigation of the comb spectral width and show how it can be optimized to obtain its maximum value defined by the laser gain bandwidth. The interplay of nonoptimal values of the resonant Kerr nonlinearity and cavity dispersion can lead to significant narrowing of the comb spectrum and reveals the best approach for dispersion compensation. The implementation of high mirror losses is shown to be favorable and results in proliferation of the comb sidemodes. Ultimately, injection locking of QCLs by modulating the laser bias around the round trip frequency provides a stable external knob to control the frequency-modulated comb state and recover the maximum spectral width of the unlocked laser state.

Published by The Optical Society under the terms of the [Creative Commons Attribution 4.0 License](https://creativecommons.org/licenses/by/4.0/). Further distribution of this work must maintain attribution to the author(s) and the published article's title, journal citation, and DOI.

<https://doi.org/10.1364/OL.424164>

Optical frequency combs (OFCs) are light sources whose spectra consist of equidistant modes with a defined phase relation [1,2]. They facilitate numerous achievements such as spectroscopy down to attosecond resolution [3], frequency synthesis and optical clocks [4], and the search for exoplanets [5]. The mid-infrared spectral region is important for spectroscopic applications, since fundamental rotation-vibrational lines of many molecules are located there [6]. Conventional OFC sources in this region depend on a chain of optical components, which limits their usability and potential for on-chip integration. To broaden the spectroscopic applications of such mid-infrared combs, a compact and electrically driven OFC generator is preferred. Quantum cascade lasers (QCLs) are unipolar semiconductor lasers that emit in the mid-infrared and terahertz ranges, which became the dominant light sources in these spectral regions [7]. In 2012, the first QCL frequency

comb was demonstrated by Hugi *et al.* [8]. Unlike conventional OFCs that rely on the emission of short pulses, QCL combs produce frequency-modulated (FM) output with an almost constant intensity and a linear frequency chirp. Moreover, the OFC regime in a free-running QCL is self-starting and requires no additional optical elements, which has led to broad attention from researchers recently [8,9]. Due to their on-chip integration, QCLs have vast potential to miniaturize high-precision spectroscopy. Mid-infrared dual-comb spectroscopy based on QCLs [10] was demonstrated, and the viability of this technique for real-time monitoring of chemical reactions was proven [11,12]. Furthermore, injection of a microwave signal at the cavity round trip frequency enables locking of the repetition rate of a QCL [13], which allows coherent control of the FM comb states using established radio-frequency (RF) electronics [14]. Recent research in this field demonstrated FM frequency comb formation in other laser types as well, e.g., interband cascade lasers [15], quantum dot lasers [16], and laser diodes [17]. The missing essential step towards the broadband high-precision spectroscopic application of QCLs is a reliable control of the FM comb states and enhancement of their optical bandwidth. The dispersion of QCL waveguides was early on identified to play an important role for FM comb formation. A prevailing method to tune the group velocity dispersion (GVD) is the use of a Gires-Tournouis etalon, where a planar mirror is placed behind the facet of the laser to induce a wavelength dependent group delay [18,19]. A different approach relies on the coupling of the dielectric waveguide to a plasmonic resonance to decrease the waveguide dispersion [20]. The experimental observations of FM combs in QCLs have mostly been found in lasers with rather small GVD, which led to the reasonable conclusion in the community that full dispersion compensation is a necessary requirement [19,21]. However, recent theoretical work revealed the key role of the interplay of multiple effects in FM comb formation, such as the GVD, Kerr nonlinearity, intracavity light intensity profile, and other effects as explained in [22,23]. It was shown that full compensation of dispersion does not necessarily lead to broader comb spectra covering the entire available gain bandwidth or a comb operation at all.

In this Letter, we show several ways of how FM combs can be optimized to increase their optical bandwidth. The presented guideline explains the roles of the GVD and resonant Kerr nonlinearity with a numerical study and reveals the impact of

the cavity facet reflectivities. All sets of optimal parameters lead to the same maximum spectral width, which is predefined by the gainwidth of the laser active medium. A theoretical analysis of the maximum bandwidth of QCL frequency combs is presented in [24]. We further present the numerical and experimental proof that the same maximal width can also be achieved by RF modulation of the injected current. This constitutes an appealing alternative to spectral width optimization, which does not require a redesign or adaptation of the laser. In a GVD compensated cavity, the laser modes are innately equidistant, which seemingly facilitates mode-locking and frequency comb formation. While this is the case for traditional mode-locked lasers that emit short pulses, the situation is very different in the case of FM comb operation. The linear frequency chirp observed for FM comb operation is the result of a complex synchronization phenomenon among the beatings of neighboring comb modes, analogous to anti-phase synchronization among coupled clocks [16]. Due to the ultrafast gain recovery time of QCLs, the spectral gain asymmetry due to Bloch gain yields a giant Kerr nonlinearity [22,25]. This induced resonant nonlinearity alters the optimal comb conditions, which is the reason that FM combs have mostly been found in GVD compensated cavities [20]. Figure 1 shows the dependence of the intensity spectrum on Kerr nonlinearity for a dispersion compensated QCL with uncoated identical facets. The simulation is based on the master equation, which considers spatial hole burning, dispersion, and Kerr nonlinearity [22]. The laser was simulated to operate well above the laser threshold, with the injection current 1.5 times larger than the threshold value. A detailed list of simulation parameters is in Supplement 1. We calculate the autocorrelation between two temporally separated round trips of the laser intensity, where the value of unity indicates a comb state and smaller values indicate unlocked states. Three different regimes can be distinguished depending on the Kerr nonlinearity. Starting from zero nonlinearity, the laser is unlocked and emits a broad spectrum. Above a threshold minimum value of the nonlinearity (around $\beta_2 = 35 \text{ pm/V}^2$), FM comb operation is obtained. Intriguingly, a further increase in Kerr nonlinearity leads to a significant narrowing of the spectrum, while the

laser remains in the locked state up to $\beta_2 = 165 \text{ pm/V}^2$. In the optimal case (35 pm/V^2), an FM comb is obtained with the broadest possible spectral width, while for a non-optimal case (chosen to be 87.5 pm/V^2 to match the spectral width of the experimental free-running comb), the laser emits a much narrower spectrum. As the Kerr nonlinearity originates from the resonant optical transitions and asymmetry of the gainshape, it is determined by the band structure design [25]. Consequently, further optimization would require a complete redesign of the active region to attain the optimal and maximal spectral width. In the following, we will discuss three alternative ways to recover the widest possible spectrum starting from the non-optimal active region (87.5 pm/V^2).

Dispersion engineering can be applied to tune a laser towards optimal FM operation, as shown above for a dispersion compensated cavity with a nonlinearity of $\beta_2 = 35 \text{ pm/V}^2$. However, for different nonlinearities, a specific non-zero GVD value will result in the largest spectral span. In Fig. 1(b), we display the numerical simulation results for the non-optimal Kerr nonlinearity of $\beta_2 = 87.5 \text{ pm/V}^2$, while sweeping the GVD from $-6000 \text{ fs}^2/\text{mm}$ to zero. By tuning the GVD from zero to $-1500 \text{ fs}^2/\text{mm}$, the same maximal spectral span can be recovered as in the case of $\beta_2 = 35 \text{ pm/V}^2$. The interplay of non-zero GVD and Kerr nonlinearity mimics the same effect on the FM comb spectral output. A further increase in GVD leads to an unlocked state and then again to a locked state with decreasing spectral span.

A novel second approach for comb engineering is the use of coatings on the facets, which changes their reflectivities. In a Fabry–Perot laser cavity, the intensities of the left and right propagating components of the field inside the cavity are increasing as they propagate, since the facets are semi-transparent. The slope of the intensity has a crucial impact on the FM comb operation, which can consequently be altered by simply changing the coatings of the laser facets [22,23]. Figure 2(a) displays a colormap of the calculated autocorrelation of the laser field from one facet. The autocorrelation in this context means that we compare the emitted intensity over one

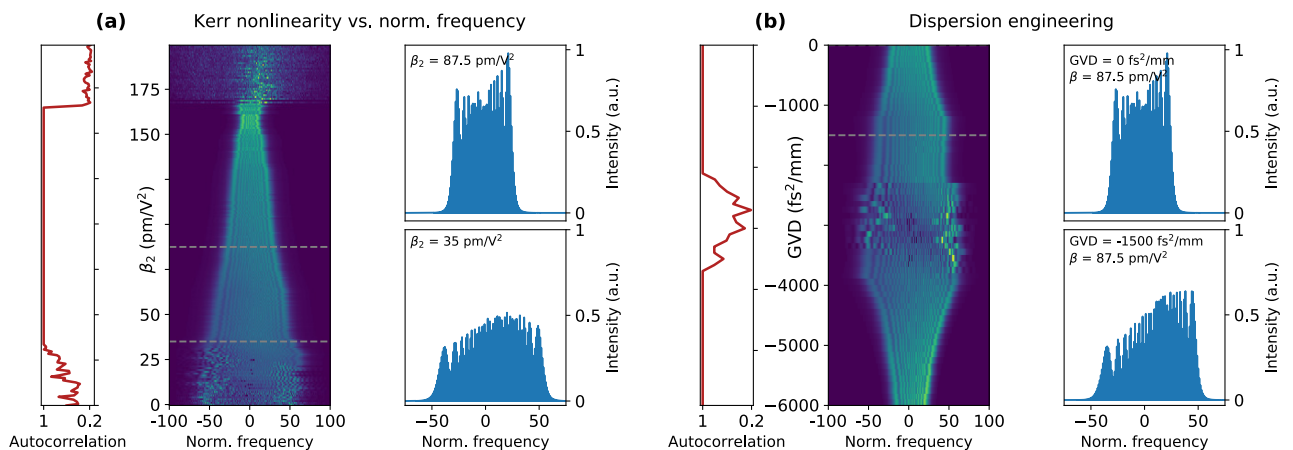


Fig. 1. (a) Evolution of the intensity spectrum with the increase in resonant Kerr nonlinearity β_2 for a dispersion compensated cavity (GVD = 0). Small β_2 leads to unlocked states, indicated by the autocorrelation value smaller than unity. FM comb formation appears between $\beta_2 = 35$ and 165 pm/V^2 with the autocorrelation equal to unity. Increase in Kerr nonlinearity narrows the spectrum. Unlocked states are obtained above $\beta_2 = 165 \text{ pm/V}^2$. Two insets on the right depict spectra taken at $\beta_2 = 35 \text{ pm/V}^2$, with maximum spectral width and at 87.5 pm/V^2 , with smaller number of comb modes. (b) Evolution of the spectrum for $\beta_2 = 87.5 \text{ pm/V}^2$ as the GVD is tuned. The maximum optical bandwidth is recovered for GVD of $-1500 \text{ fs}^2/\text{mm}$ or $-4000 \text{ fs}^2/\text{mm}$.

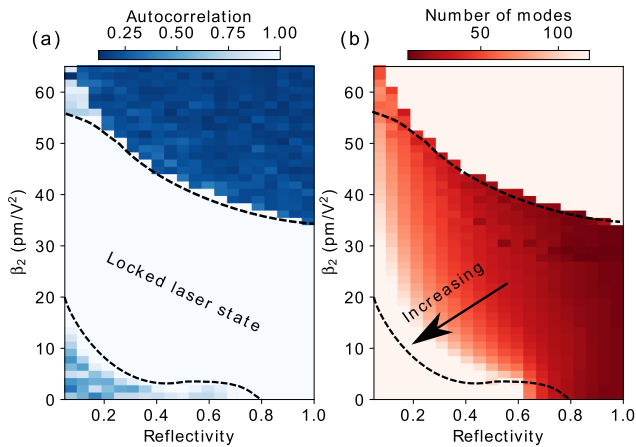


Fig. 2. (a) Calculated autocorrelation as both the Kerr nonlinearity and reflectivity of one cavity facet are tuned, while the reflectivity of the other facet is set to one. FM comb formation is obtained in the region between the black dashed lines. (b) Calculated spectral width for the same parameter sweep. Optimal region with the largest number of comb modes is indicated with the arrow. Relevant data where an FM comb is obtained lies between the black dashed lines.

round trip with the emitted intensity delayed by 450 round trips. In a comb, they match perfectly, and the autocorrelation is exactly unity. We sweep the reflectivity for one facet from zero to one with the other facet reflectivity set to one, while sweeping the Kerr nonlinearity from $\beta_2 = 0$ to 65 pm/V^2 . The asymmetry is optimal in terms of output power and efficiency, but is not particularly relevant for FM comb operation.

A large part of the parameter space is a locked FM comb state (indicated by the dashed lines). There are two areas of unlocked states when both the Kerr nonlinearity and facet reflectivity are either low or relatively large. If the comb does not lock for low values of nonlinearity, it can be brought into the locked regime by increasing the facet reflectivity. Conversely, for too high nonlinearities, the reflectivity needs to be decreased. In Fig. 2(b), we show the corresponding spectral width to identify regions where the comb is characterized with a broad intensity spectrum. Evidently, an optimal condition for a locked laser state with the broadest spectral output is obtained with a small reflectivity (close to the lower dashed line). One can see that the

overlap for optimal conditions, a broad spectrum and locked laser state, is small compared to the size of the locking area in Fig. 2(a). Furthermore, as nonlinearity is determined by the design of the laser active region, only the reflectivity value can be tuned. Note that due to the interplay of the GVD and Kerr nonlinearity, dispersion engineering affects the comb state similarly as changing the nonlinearity in Fig. 2(a). Our results emphasize that changing the reflectivity of the laser facet can serve as a practical way to impact the FM comb operation, particularly as coating technology is already a part of laser fabrication.

As a third approach, we present a technique that does not require precise adjustment of the cavity for a specific active region—the injection of an RF signal around the cavity round trip frequency. To model the influence of the modulation of the injection current on the spectrum of FM combs, we again employ the coherent master equation [22,26]. We furthermore provide an experimental proof, similar to recent work [27]. The laser has the same non-optimal Kerr nonlinearity of 87.5 pm/V^2 and zero GVD. The current modulation is applied to a short section that covers 10% of the laser cavity. In Figs. 3(a) and 3(b), we show the intensity spectrum and phase differences of neighboring modes of the FM comb, both analyzed with and without current modulation. Without modulation, the comb spectrum spans over 74 modes. The intermodal phase differences are linearly splayed over the full range of 2π , which is characteristic for FM combs and results in a linear frequency chirp. The lower plot in Fig. 3(a) shows the optical spectrum when the laser is subjected to strong current modulation with an amplitude of 10% of the DC driving current. With RF modulation, the comb spectrum significantly broadens from 74 to 134 modes. The slope of the intermodal phase differences in Fig. 3(b) broadens accordingly and flattens out, demonstrating the locked coherent behavior of the FM comb state. We experimentally investigated the predicted behavior with a high performance mid-infrared QCL frequency comb emitting at $8 \mu\text{m}$. The QCL cavity is split into a 3.15 mm long gain section and a $350 \mu\text{m}$ short modulation section optimized for efficient RF injection. Besides the optimized RF geometry of the modulation section, the band structure of the QCL active material was designed as a single stack bifunctional active region [26,28]. When operated at zero-bias, the QCL works as a detector at its lasing wavelength and thus induces strong optical absorption. This allows a more efficient modulation of the laser with larger

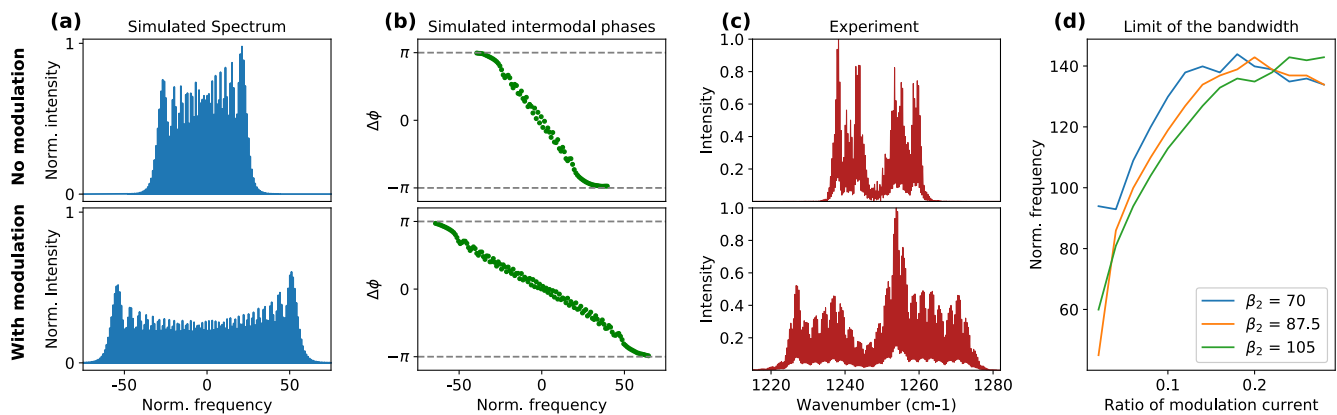


Fig. 3. Simulated (a) intensity spectrum and (b) intermodal phase differences with (bottom) and without (top) modulation of the injection current. (c) Experimental intensity spectrum with (bottom) and without (top) modulation of the injection current. (d) Simulated spectral width depending on modulation depth.

modulation depths. To study the response of the QCL combs spectrum, we operate the modulation section at a DC bias of 2.8 V to maximize the modulation efficiency. The modulation power is increased continuously up to 35 dBm injection power. The large modulation power is provided by a mini circuits ZVE-3W-183+ power amplifier. From the 35 dBm, a significant fraction (15 dB) is lost by the remaining parasitic capacitance of the QCL. A detailed characterization of the modulation capabilities using a rectification experiment [29], as well as an estimation of the effective modulation depth can be found in Supplement 1. The associated optical output spectrum is displayed in Fig. 3(c). The spectrum of the free running QCL shows an optical bandwidth of 30 cm^{-1} without any modulation. When injecting RF power at the round trip frequency of the free running laser, the spectrum is broadened to 50 cm^{-1} . This experimental proof shows that RF injection can not only be used to stabilize the FM comb [14], but also to optimize the FM comb state and recover its maximum spectral width, which is defined by the laser gainwidth. All three presented methods gave a similar spectral width under optimal conditions for the FM comb. To further explore this upper limit, we provide a more detailed study of the spectral broadening by RF modulation. We simulated the spectral broadening depending on the modulation depth ($I_{\text{RF}}/I_{\text{DC}} = 0-0.3$) for fixed values of Kerr nonlinearity of 70, 87.5, and $105 \text{ pm}/V^2$ and an injection frequency 10 MHz below the cold cavity round trip time. The results are displayed in Fig. 3(d). For all values of the nonlinearity, the simulated behavior is strikingly similar. The spectral width increases considerably up to a modulation depth of 0.15, where it saturates at an approximately constant bandwidth of 140 modes. The maximal optical bandwidth achievable by RF modulation is practically equal to the width of the unlocked state. This result shows that the spectral width of the FM comb does not exceed the width of the unlocked laser [24,27].

In conclusion, we provided a guideline to engineer FM combs for broadband spectroscopic application. We investigated the influence of multiple cavity parameters of FM combs by using numerical models and provided a proof-of-concept experiment. Due to the inherent resonant Kerr nonlinearity of the QCL active region, strictly reducing and compensating for the GVD does not result in an optimal frequency comb regime, in contrast to previous expectations. The profile of the intracavity light intensity has a crucial role in FM comb formation. It can be controlled by tuning the laser facet reflectivities to broaden the comb spectra. Moreover, we demonstrate that high mirror losses are preferable. Employing a sophisticated model using the master equation approach, we simulate the FM comb response to a strong modulation of the injection current around the cavity round trip frequency. The experiment with an injection locked high performance bifunctional QCL frequency comb displays excellent agreement with the modeled behavior. To overcome the restrictions that are dominantly imposed by the laser design, RF injection is the method of choice to circumvent the change of the laser active region and achieve a broad spectral output with reasonable effort. The further use of RF modulation as an efficient technique to broaden the spectrum of the FM comb will enhance QCL applications in dual-comb spectroscopy.

Funding. Austrian Science Fund (P28914); H2020 European Research Council (853014).

Disclosures. The authors declare no conflicts of interest.

Data Availability. Data underlying the results presented in this paper are not publicly available at this time but may be obtained from the authors upon reasonable request.

Supplemental document. See Supplement 1 for supporting content.

†These authors contributed equally to this Letter.

REFERENCES

1. T. W. Hänsch, *Rev. Mod. Phys.* **78**, 1297 (2006).
2. J. L. Hall, *Rev. Mod. Phys.* **78**, 1279 (2006).
3. A. Baltuška, T. Udem, M. Uiberacker, M. Hentschel, E. Goulielmakis, C. Gohle, R. Holzwarth, V. S. Yakovlev, A. Scrinzi, T. W. Hänsch, and F. Krausz, *Nature* **421**, 611 (2003).
4. T. Udem, R. Holzwarth, and T. W. Hänsch, *Nature* **416**, 233 (2002).
5. T. Wilken, G. L. Curto, R. A. Probst, T. Steinmetz, A. Manescau, L. Pasquini, J. I. G. Hernández, R. Reboło, T. W. Hänsch, T. Udem, and R. Holzwarth, *Nature* **485**, 611 (2012).
6. F. Keilmann, C. Gohle, and R. Holzwarth, *Opt. Lett.* **29**, 1542 (2004).
7. J. Faist, F. Capasso, D. L. Sivco, C. Sirtori, A. L. Hutchinson, and A. Y. Cho, *Science* **264**, 553 (1994).
8. A. Hugi, G. Villares, S. Blaser, H. C. Liu, and J. Faist, *Nature* **492**, 229 (2012).
9. M. Singleton, P. Jouy, M. Beck, and J. Faist, *Optica* **5**, 948 (2018).
10. G. Villares, A. Hugi, S. Blaser, and J. Faist, *Nat. Commun.* **5**, 5192 (2014).
11. J. L. Klocke and T. Kottke, *Phys. Chem. Chem. Phys.* **22**, 26459 (2020).
12. N. H. Pinkowski, Y. Ding, C. L. Strand, R. K. Hanson, R. Horvath, and M. Geiser, *Meas. Sci. Technol.* **31**, 055501 (2020).
13. M. R. St-Jean, M. I. Amanti, A. Bernard, A. Calvar, A. Bismuto, E. Gini, M. Beck, J. Faist, H. C. Liu, and C. Sirtori, *Laser Photon. Rev.* **8**, 443 (2014).
14. J. Hillbrand, A. M. Andrews, H. Detz, G. Strasser, and B. Schwarz, *Nat. Photonics* **13**, 101 (2018).
15. B. Schwarz, J. Hillbrand, M. Beiser, A. M. Andrews, G. Strasser, H. Detz, A. Schade, R. Weih, and S. Höfling, *Optica* **6**, 890 (2019).
16. J. Hillbrand, D. Auth, M. Piccardo, N. Opačak, E. Gornik, G. Strasser, F. Capasso, S. Breuer, and B. Schwarz, *Phys. Rev. Lett.* **124**, 023901 (2020).
17. L. A. Sterczewski, C. Frez, S. Forouhar, D. Burghoff, and M. Bagheri, *APL Photon.* **5**, 076111 (2020).
18. J. Hillbrand, P. Jouy, M. Beck, and J. Faist, *Opt. Lett.* **43**, 1746 (2018).
19. G. Villares, S. Riedi, J. Wolf, D. Kazakov, M. J. Süess, P. Jouy, M. Beck, and J. Faist, *Optica* **3**, 252 (2016).
20. Y. Bidaux, I. Sergachev, W. Wuester, R. Maulini, T. Gresch, A. Bismuto, S. Blaser, A. Müller, and J. Faist, *Opt. Lett.* **42**, 1604 (2017).
21. D. Bachmann, M. Rösch, G. Scalari, M. Beck, J. Faist, K. Unterrainer, and J. Darmo, *Appl. Phys. Lett.* **109**, 221107 (2016).
22. N. Opačak and B. Schwarz, *Phys. Rev. Lett.* **123**, 243902 (2019).
23. D. Burghoff, *Optica* **7**, 1781 (2020).
24. J. B. Khurgin, *Appl. Phys. Lett.* **117**, 161104 (2020).
25. N. Opačak, S. D. Cin, J. Hillbrand, and B. Schwarz, "Frequency comb generation by Bloch gain induced giant Kerr nonlinearity," arXiv:2102.08167 (2021).
26. J. Hillbrand, N. Opačak, M. Piccardo, H. Schneider, G. Strasser, F. Capasso, and B. Schwarz, *Nat. Commun.* **11**, 5788 (2020).
27. F. Kapsalidis, B. Schneider, M. Singleton, M. Bertrand, E. Gini, M. Beck, and J. Faist, *Appl. Phys. Lett.* **118**, 071101 (2021).
28. B. Schwarz, P. Reininger, H. Detz, T. Zederbauer, A. Maxwell Andrews, S. Kalchmair, W. Schrenk, O. Baumgartner, H. Kosina, and G. Strasser, *Appl. Phys. Lett.* **101**, 191109 (2012).
29. B. Hinkov, A. Hugi, M. Beck, and J. Faist, *Opt. Express* **24**, 3294 (2016).